Supported and unsupported platinum catalysts prepared by a one-step dry deposition method and their oxygen reduction reactivity in acidic media

Justin Roller · Roberto Neagu · Frank Orfino ·
Radenka Maric

Abstract The present study examines the physical and electrochemical properties of platinum particles generated by a combustion method for use in oxygen reduction on the cathode side of a proton exchange fuel cell (PEMFC). This method employs a one-step, open-atmosphere, and dry deposition technique called reactive spray deposition technology (RSDT). The objective of this study is to characterize the intrinsic activity of the platinum produced for incorporation into low-loading cathode electrodes in high performing membrane electrode assemblies (MEA). The process allows for independent real-time control of the carbon, platinum, and ionomer ratios in the final electrode. In this research work we examine the oxygen reduction reaction via a rotating disk three electrode set-up to understand the intrinsic activity of the as-sprayed platinum as well as platinum condensed onto a carbon support. The mass and specific activities were measured in a 0.1 M perchloric acid electrolyte under different deposition conditions and loading was verified by atomic emission spectroscopy inductively coupled plasma (AES-ICP). Microscopy results indicate that the platinum particle sizes are 5 nm ($\sigma = 2.8$ nm) in diameter while TEM and XRD show that the platinum generated by the process is pure and crystalline without bulk oxides or precursor material present. The initial rotating disk electrode result shows that the RSDT technique is capable of producing catalysts with an oxygen reduction mass activity at 0.9 V of 200 mA/mg$_{Pt}$ rotating at 1600 rpm and 30 °C. The electrochemically active surface area approaches 120 m^2/g for the platinum, carbon, and ionomer samples and the unsupported sample with only platinum has an active area of 92 m^2/g. The rather larger surface area of the unsupported sample exists when the platinum is deposited as a highly porous nanostructured layer that allows for high penetration of reactant.

Introduction

The deposition of platinum nanoparticles from the vapor phase through an open atmosphere combustion processes has been explored by relatively few researchers [1–4]. The application of this type of process to directly depositing onto electrolytes or GDLs for proton exchange fuel cell (PEMFC) applications is even more limited [1, 5–10]. Production of platinum catalysts via a flame mechanism holds promise as a one-step production process for very low Pt catalyst (<0.1 mg/cm^2) on the cathode. This preparation method will by-passes traditional ink preparation routes in order to reduce platinum loading to the Department of Energy motive target (0.125 g/kW) while independently controlling Pt, ionomer, and support loading. High surface area fuel cell catalysts are often synthesized from halide-containing counter ions (e.g. Cl$^-$), which are not always completely removed after synthesis and chloride can be a likely contaminant. In the reactive spray deposition technology (RSDT) synthesis route, solid platinum nanoparticles are grown from the vapor phase without any halide containing precursors as described elsewhere [11]. In this process the metal organic solute, platinum 2,4-pentanedionate, is dissolved into toluene in a

J. Roller (✉) · R. Maric
Department of Chemical Materials & Biomolecular Engineering, Center for Clean Energy Engineering, University of Connecticut, Storrs, CT, USA
e-mail: Justin.roller@engr.uconn.edu

R. Neagu · F. Orfino
National Research Council-Institute for Fuel Cell Innovation, Vancouver, BC, Canada

sealed vessel and further diluted with liquefied propane. This solution is then pumped into an atomizing nozzle and the resultant droplets are ignited by a ring of burners. The spray generated by this nozzle is formed by a combination of pressure, heat, and supercritical atomization. The spray forms very small droplets less than 1 μm in diameter. Once ignited, the solvent burns off and the solute is left in a concentrated core at which point the temperature rises to decompose the organic ligand with the platinum. This is followed by melting and ultimately vaporization of the platinum in the reaction zone of the flame. In order to study the intrinsic activity of the platinum produced by this flame based process, a series of depositions directly onto glassy carbon electrodes was undertaken. First the deposition was with platinum only without support and ionomer, and then with platinum, Nafion, and carbon support.

The development of high utilization, low Pt loading catalysts requires quantitative determination of electrocatalytic activity under conditions relevant to fuel cell operation. Except for start-up and shut-down this generally means a continuous reactant flow at a temperature of 60–80 °C. In general, manufacturing a membrane electrode assembly as used in a working fuel cell introduces many more unknowns and greatly adds to the difficulty in determining the intrinsic catalyst performance. This is because, there are uncertainties related to mass transport resistances such as gas flow impediment from flow field design or crushing of the catalyst layer (CL) due to improper gasket choice and over torquing. In addition, there can be issues related to water management since the CL requires an optimal humidity that balances the need for ionic conductivity in the impregnated Nafion® and the diffusion of oxygen through the entire layer so that platinum utilization is maximized. In addition, the conversion of chemical to electrical energy in the cell generates a large amount of water that can flood the pores and decrease oxygen diffusion. All of these complex effects make decoupling the intrinsic activity of the catalyst more challenging. In tradition, the way to overcome this limitation is by the use of a rotating disk electrode (RDE) experiments.

For ink based production routes a catalyst is usually dispersed in an aqueous suspension aided by sonication. Precisely known amounts of the aqueous suspensions are then pipetted onto a glassy (non-graphitized) carbon disk and dried. Following the drying step, a dilute solution of a proton conducting polymer, i.e. Nafion®, is added to act as a binder. The total thickness of the catalyst/Nafion layer should be well below the diffusion layer on a RDE at the rotation speeds used for the experiment. The novelty in the RSDT approach is that the catalyst layer is dry deposited under the same conditions and in the same manner as when deposited onto the Nafion membrane for membrane electrode assembly (MEA) testing. In this way the electrode is directly dry deposited onto the glassy carbon electrode in

one-step and analyzed as produced. This mimics directly the conditions of the layer formed when making a MEA for testing. The same conditions for RDE testing are not met when they are pipetted from a slurry and dried directly onto a glassy carbon electrode versus sprayed or screen printed when making a MEA.

Experimental

Depositions by the RSDT process onto electrodes were done directly and in triplicate by thermal decomposition and desublimation of platinum (II) 2,4-pentanedionate (Colonial Metals) dissolved in a toluene/propane mixture and passed through the atomization and quenching sections of the RSDT process. The carbon support used in this study was EC-300 J Ketjen black (Akzo Nobel) and a 5 wt% Nafion ionomer solution (EW1000, DuPont) was added so as to provide 30–40 wt% Nafion in the CL. The mixture was homogenized by sonication using a Misonix Sonicator 3000 (QSonica, LLC) for 1 h using a 2 s pulse followed by a 2 s rest routine at an output level of 4. Carbon support and ionomer were sprayed into the RSDT reaction zone using low volume low pressure 781S-SS-28F slurry nozzles (EFD, Nordson Co.). The RSDT system was used to deposit either platinum or a platinum/carbon/ionomer mixture onto a hands-free 5 mm OD glassy carbon disk and assembled in a AFE6 M shaft (Pine Instruments, Raleigh NC) for use as the working electrode. The RSDT process is described in more detail in Ref. [11].

In order to investigate the microstructure of the electrodes at the particle level and to confirm their suitability for electrochemical tests, a polypropylene test coupon was also deposited on simultaneously. Image of the surface morphology were examined by scanning electron microscopy (SEM) using both Hitachi S-3500 N and a FEI Helios NanoLab dual beam microscopes. Small pieces of sample were cut off the polypropylene coupons and prepared for TEM investigations as well as having 1″ diameter circles punched out for XRD analysis. Cut-off sections from the coupon were embedded in an Araldite 502 resin (SPI supplies) and cured at 100 °C. 80–100 nm thin cross sections were cut with a microtome (Leica Ultracut T) using a Diatome Ultra, 4 mm, 45° standard Al boat diamond knife (Diatome) and were investigated with a TEM (Hitachi H7600) using 100 kV acceleration voltage. Phase identification and crystallite size were obtained with a D8 Advance X-ray diffractometer (Bruker-AXS, Madison, WI) using a Cu-anode at a wavelength of 0.154 nm with a power setting of 40 kV at 40 mA. All electrochemical measurements were performed in a three electrode, single-compartment half-cell with the reference electrode (RE) as a reversible hydrogen electrode (RHE) (Sandfire Scientific

Ltd.). A platinized mesh was used as the auxiliary or counter electrode (CE). All potentials reported in this article are relative to a RHE immersed in 0.1 M HClO$_4$ at 30 °C. Cyclic voltammetry was performed using a Solartron Multistat 1480, controlled with CorrWare software (Scribner). Rotating disk voltammetry was performed using an ASR rotator (Pine Instrument Co.). The whole half-cell was immersed in a temperature controlled water bath (Fisher Isotemp 205) covered with insulating plastic balls to minimize temperature fluctuations and evaporation.

In this set of experiments the electrodes were first placed in the electrolyte without rotation and N$_2$ was bubbled in the cell for 30 min to reach saturation. The open circuit potential (OCP) was recorded to ensure stability. The electrode was then cycled 10 times (100 mV/s) between 0.0–1.2 V to clean the electrode surface and check for stability. Following this treatment, the electrode was scanned 20 times from 0.05–1.1 V at 10 mV/s and the 20th scan was used to measure the electrochemically active surface area. After this the N$_2$ was replaced with O$_2$ and allowed to bubble in the electrolyte for 30 min, without rotation of the electrode. Once a stable OCP in O$_2$ was recorded the electrode was rotated at 1600 rpm and scanned from OCP (1.01–1.05 V) to 0.3 V at 5 mV/s for five scans. At the end of the 5th scan, the electrode was then scanned one time and on the anodic scan the kinetic and diffusion limited currents were recorded at 0.9 and 0.3 V, respectively. A detailed description of the experimental approach has been described elsewhere [12–14].

Results

In order to appropriately determine the bulk phase of the deposited material, test coupons of representative samples were analyzed by XRD. The platinum (II) 2,4-pentanedionate precursor exists as a yellow crystalline powder with an anorthic (triclinic) lattice having the strongest peak at low angles of 2θ equal to 11.831° corresponding to the (1 0 0) plane and 13.51° corresponding to the (0 0 1) plane and does not exhibit any reflections above 34.643° as shown in ICDD card No. 50-2288. Figures 1 and 2 show, respectively the diffraction traces for representative samples consisting of platinum only and carbon supported platinum superimposed on the pattern for metallic platinum. Metallic platinum exists as a face-centered cubic structure having the strongest reflections at low angles of 2θ equal to 39.765° corresponding to the (1 0 0) plane and 46.244° corresponding to the (2 0 0) plane and does not exhibit any reflections below 39.765°.

The weak intensity and the high noise level of the diffraction patterns for the RSDT produced samples are due to the relative low loading of these samples $\sim$0.1 mg/cm^2. It
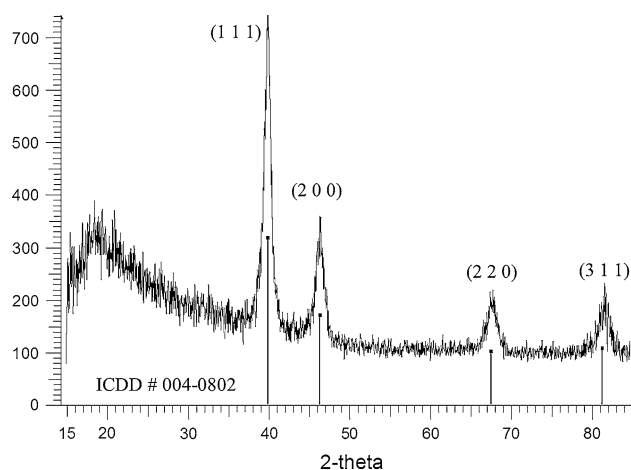

Fig. 1 Diffraction pattern of platinum metal produced by RSDT indexed to ICDD database card # 00-004-0802
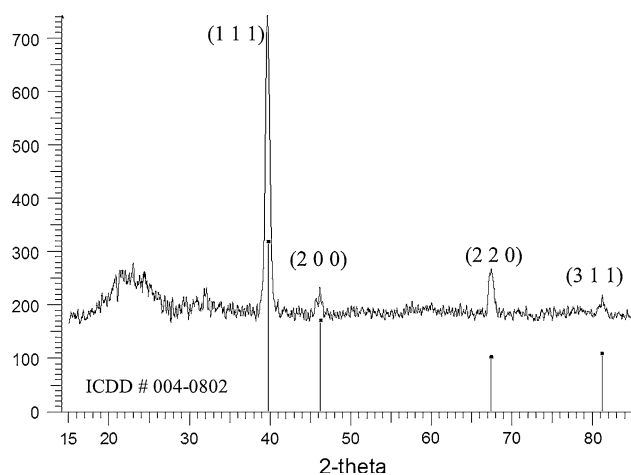

Fig. 2 Diffraction pattern of carbon supported platinum metal produced by RSDT indexed to ICDD database Card # 00-004-0802

should be noted that diffraction patterns would be too weak if analyzed on the exact samples used in each RDE experiment since the loading of those samples is over 100 times lower.

Prior to directly building the RSDT catalysts into electrodes, the platinum particles were sprayed onto a 3 mm Cu 200 mesh TEM grid (SPI, West Chester, PA) quickly inserted and then removed from the active zone of the RSDT axis at a 15 cm stand-off distance. Figure 3a shows the size and distribution of the as-sprayed platinum particles, while Fig. 3b shows the electron diffraction ring of a representative particle. Manual counting of particles on the grid gave an average particle size of 5.4 nm ($\sigma = 2.8$ nm). The diffraction pattern confirms that the particle is polycrystalline and adopts a face-centered cubic structure with the four strongest planes (1 1 1), (2 0 0), (2 2 0), and (3 1 1) well resolved.

Typical TEM micrographs of the as deposited electrode materials are shown in Fig. 4.
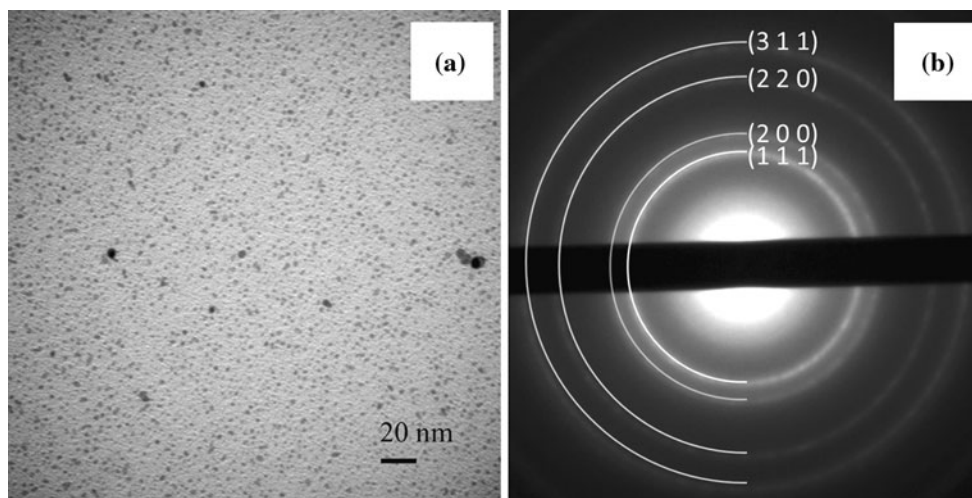
Fig. 3 Platinum particles produced by the RSDT process and collected directly onto a Cu grid at a stand-off distance of 15 cm
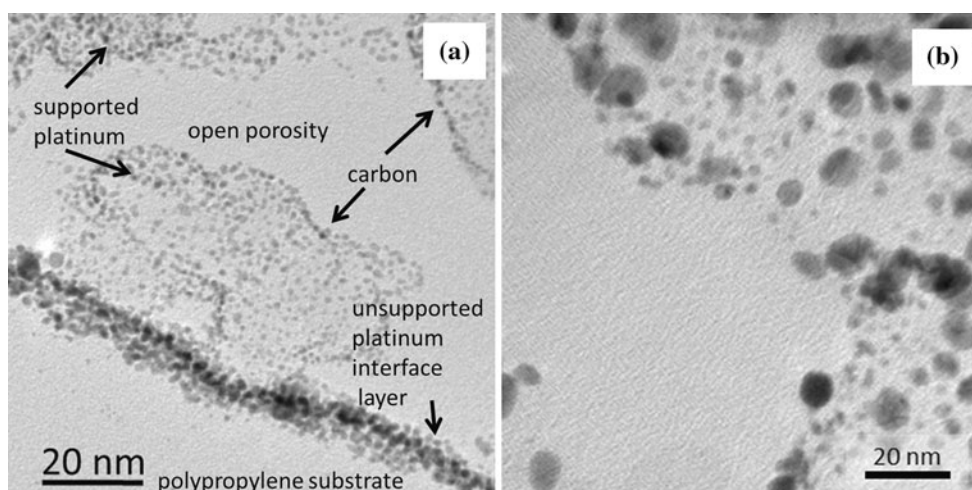

Fig. 4 Bright field TEM image of a cross section through the RSDT catalyst layers deposited on a polypropylene coupon. **a** Electrode microstructure. **b** Detail showing distribution of Pt and C particles

The TEM images confirm that the coatings have a fairly porous microstructure. Such porosity favours the penetration and access of electrolyte to catalyst particles; hence, the effect of mass transport limitations on the electrochemical performance would be negligible. A higher magnification image (Fig. 4b) details the electrode's microstructure at the scale of individual Pt and C particles. The catalyst is homogeneously distributed and, although some larger particles do exist, the vast majority of Pt is dispersed as 2–5 nm particles onto the support. We have not observed large agglomerations of Pt particles. Some undispersed agglomerates of carbon particles are seen, as suggested by similar features found in the SEM observations. Presence of carbon agglomerates should not affect the accuracy of RDE measurements and, since they are small compared to the scale of the coupons used for

loading measurements, the latter can be considered as being representative for our samples as well. Therefore, mass specific property values presented in this study should be relevant for RSDT made carbon supported Pt catalysts.

Three glassy carbon electrodes were simultaneously deposited upon by the RSDT process along with a test coupon for 15 min. For each run the coupon was submitted for atomic emission inductively coupled plasma spectroscopy (AE-ICP) analysis of platinum content. The formulation of each electrode and the results of the platinum analysis are listed in Table 1.

It is seen from Table 1 that the loading values are between 6.1 and 8.4 $\mu g/cm^2$ for the samples with platinum, carbon, and ionomer (i.e. PCI-1 to PCI-5), while the platinum only sample (PT-1) is slightly lower in loading for the same 15 min of spray. This lower deposition rate may be

Table 1 Formulation and metal content analysis for six different types of electrodes manufactured by RSDT

| Sample	Pt loading ($\mu g/cm^2_{geometric}$)	Carbon loading ($mg/cm^2_{geometric}$)	Ionomer loading ($mg/cm^2_{geometric}$)	Ionomer/carbon mass ratio	Pt/carbon mass ratio
PT-1	4.9	0	0	Pt only	NA
PCI-1	6.1	0.0340	0.0182	0.54	0.18
PCI-2	8.4	0.0326	0.0258	0.79	0.26
PCI-3	7.7	0.0258	0.0200	0.78	0.30
PCI-4	7.2	0.0287	0.0233	0.81	0.25
PCI-5	6.7	0.0422	0.0396	0.94	0.16

due to the lack of ionomer binder to hold the sprayed particles in place. PCI-1 was intentionally sprayed with a lower ionomer/carbon ratio of ~0.5 while PCI-2 to PCI-4 was intended to have an ionomer/carbon ratio of ~0.8. PCI-5 has the highest ionomer/carbon ratio at ~0.9. To ensure that the electrodes were covered evenly, a scanning electron micrograph (SEM) was taken on a Hitachi S-3500 N and checked by energy dispersive X-ray analysis (EDX) for platinum.

Once an even coating of pure platinum was confirmed, the carbon-ionomer slurry nozzles were added to inject the carbon support and ionic conducting phase into the platinum reaction plume. It is important to note that the carbon and ionomer slurry were co-injected into the plume very close to the substrate and that the temperature of the gas stream just prior to the substrate is ~100 °C. The distance from the slurry nozzles, flow rate, and atomization were adjusted so that most of the solvent evaporates prior to hitting the surface. However, there are some droplets that invariably strike the substrate surface and then evaporate immediately. If these parameters were not correctly adjusted then the slurry would strike the surface and run down the substrate, creating a streaking effect. A SEM micrograph of the ternary composite (carbon, ionomer, and platinum) using a FEI Helios NanoLab is shown in Fig. 5.

The micrograph in Fig. 5 shows that the electrode coverage is uniform with sub-micron sized porosity along with less uniform inter-dispersed macropores that range from 1 to 5 μm in size laterally. The surface of the electrode exhibits valleys that span from 10 to 20 μm laterally but overall the majority of the surface area exists as a planar structure. A closer view of the electrode is shown in Fig. 6.

The carbon particle aggregates in Fig. 6 highlight the extent of the microporosity across the electrode. The 30–60 nm primary carbon particles are fused into larger agglomerates with varying lateral width. Many of the pores appear to be open channels with little tortuosity. This open structure should facilitate fresh electrolyte reactant access to the entire depth of the electrode thickness.

Each electrode type listed in Table 1 was made simultaneously in triplicate, i.e., for each deposition a total of
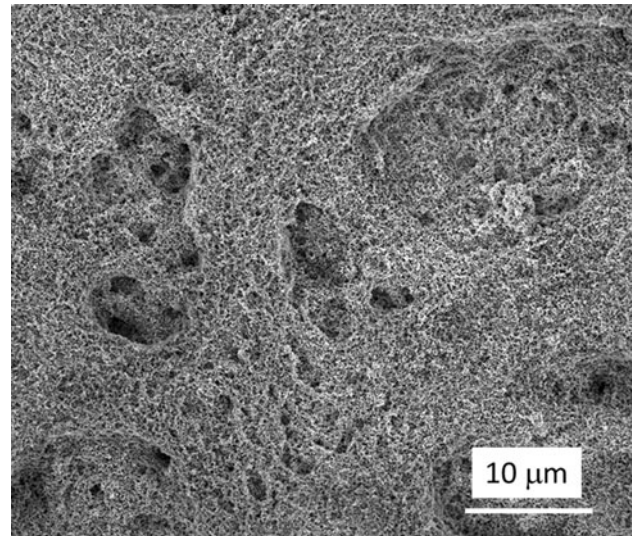
Fig. 5 SEM micrograph of sample PCI-4
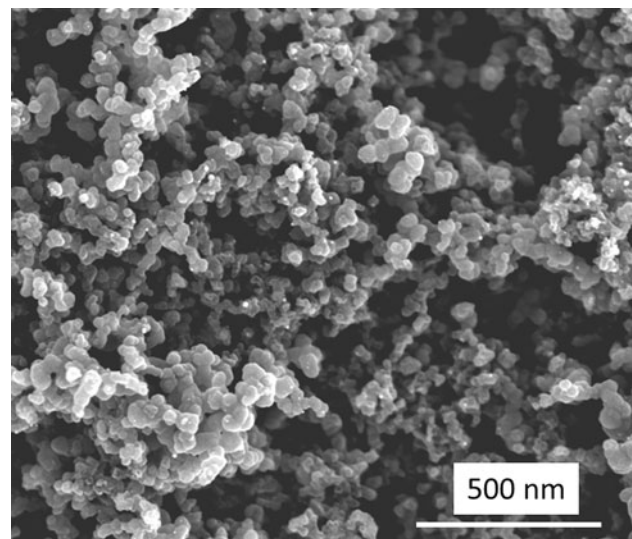
Fig. 6 SEM micrograph of sample PCI-4

three electrodes were made. The average values of the ECA are reported along with the standard of deviation, σ of the three results in Table 2:

Table 2 Roughness factor and electrochemically active surface area of RSDT electrodes in N_2 saturated 0.1 M $HClO_4$ electrolyte at a scan rate of 20 mV/s

Sample	Roughness factor r_f	Average ECA (m^2/g_{Pt})	σ ECA (m^2/g_{Pt})
PT-1	4.5	91.5	1.2
PCI-1	6.1	101.1	14.9
PCI-2	10.1	119.6	3.2
PCI-3	5.7	73.6	6.5
PCI-4	5.9	81.1	8.2
PCI-5	7.1	106.0	4.2

The ECA results calculated from the CV scans are exceptionally high compared to values of ~ 60 m^2/g_{Pt} encountered in the literature for Pt dispersed on carbon. The ICP-AES loading results were consistent with our gravimetric determination of platinum loading. An ECA value of 100 m^2/g_{Pt} corresponds to an average particle size of 2.8 nm [15].

The CV scans for determination of the ECA values of the composite samples are shown in Fig. 7. The legend at the right shows the order of the scans with the highest current density at 1.2 V being PCI-2 and the lowest being PCI-3. A representative CV scan to compare the platinum only electrode with a composite electrode is shown in Fig. 8.

It can be seen in Figs. 7 and 8 that the as-sprayed electrodes do indeed exhibit the typical behavior toward hydrogen adsorption/desorption where the three redox peaks, corresponding to multiple low index crystallographic phases of Pt are observed. In general, the CV scans reached a repeatable trace after only several cycles during the conditioning phase of the measurement. The scans are a little noisy and this was found, after the fact, to be due to interference of the magnetic stirrer used for the temperature bath. A look at PCI-5 shows how steady the traces were
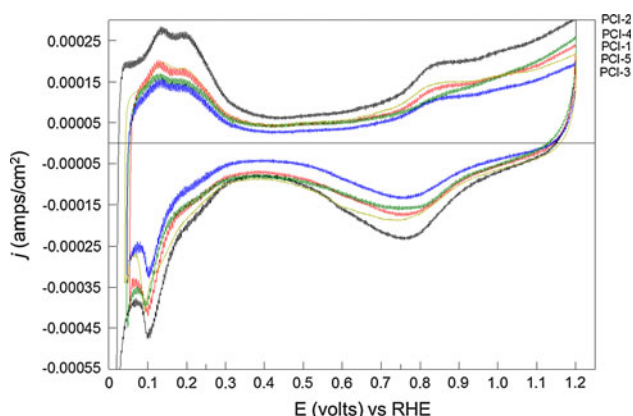
Fig. 7 Representative CV of each composite RSDT electrode in N_2 saturated 0.1 M $HClO_4$ at 30 °C using a scan speed of 10 mV/s
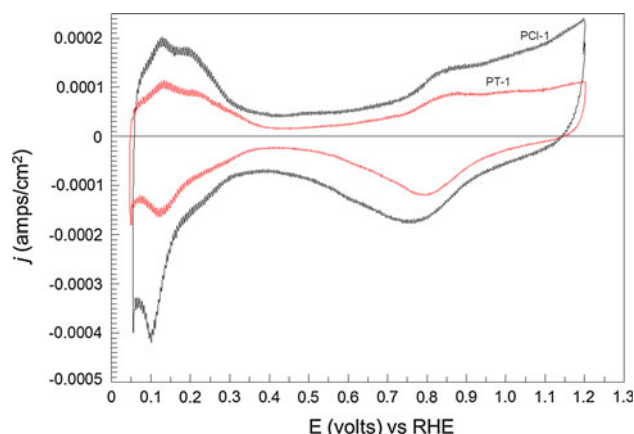
Fig. 8 Representative CV of a composite versus a platinum only RSDT electrode in N_2 saturated 0.1 M $HClO_4$ at 30 °C using a scan speed of 10 mV/s

once the stirrer was turned off while the other scans exhibit noisier traces.

There does not seem to be a linear relationship between loading and the adsorption/desorption current, but since the loadings are very small and the differences less than 2 μg/cm² between samples it is not surprising that there is some discrepancy. Sample PCI-2 with the highest platinum loading of 8.4 μg/cm² and an ionomer/carbon ratio of 0.79 did indeed show the largest adsorption/desorption current as shown in Fig. 10. What is perhaps the most surprising is that the platinum only sample, PT-1 had the lowest loading 4.9 μg/cm² and yet the hydrogen adsorption/desorption current was higher than two of the supported catalysts. This is only possible if the platinum was deposited as a very porous network as we have shown previously [9]. In addition, it should be noted that the carbon support particles are known to be 30–50 nm in primary particle size which then form larger agglomerates that are a function of the type of carbon and the method of manufacture. The platinum particles that are generated by RSDT are on the order of a few nanometers [5]. Thus the platinum forms a very thin layer on the electrode that is just as electrochemically accessible as the dispersed platinum. Achieving a platinum film morphology in which the surface area to volume ratio is very high, while still having channels for reactant gases and product water to be exchanged, would eliminate the need for a dispersant support assuming that the electrical conductivity was sufficient between the nanosized crystals. This suggests that research into thin electrodes may lead to higher platinum utilization in the cathode as has been suggested by Eikerling et al. [16].

After completing the final CV scan, the N_2 was removed and replaced with O_2 from the cell and allowed to saturate for 1 h. The rotator was set to 1600 rpm and both the anodic diffusion limited current at 0.3 V and the current at 0.9 V were recorded. From this data the mass and specific

Table 3 Average kinetic and diffusion limited current density values for each electrode composition and the calculated values of mass activity, i_m, and specific activity, i_s

Sample	j_k at 0.9 V (mA/cm^2 geometric)	σj_k (mA/cm^2 geometric)	j_d at 0.3 V (mA/cm^2 geometric)	i_m at 0.9 V (mA/mg$_{Pt}$)	ECA (m$^2_{Pt}$/g$_{Pt}$)
PT-1	0.99	0.09	5.65	201	92
PCI-1	0.94	0.11	5.87	143	101
PCI-2	0.78	0.05	5.26	93	120
PCI-3	0.63	0.08	5.71	76	74
PCI-4	0.80	0.08	5.70	111	81
PCI-5	0.75	0.09	5.77	111	106

activities were calculated according to equations (7 and 8) as shown in Table 3.

Figure 9 shows all of the potentiodynamic scans superimposed for the composite samples PCI-1 to PCI-5 and a close up of the current density is shown in Fig. 10 for comparison. The average kinetic current density, j_k is highest for PCI-1 which also has the lowest ionomer to carbon ratio at 0.54. The kinetic current density is even higher for the platinum only sample. This suggests that there may be some mass transport deviation from the ideal RDE due to the Nafion® and this effect should be subsequently studied.

However, considering the standard of deviation, σj_k, on the measurements, and the measurement overlap at the 3σ confidence interval, it is difficult to ascertain any clear trends. Figure 11 shows the potentiodynamic ORR traces for composite (PCI-1) and platinum only (PT-1) RSDT samples for comparison.

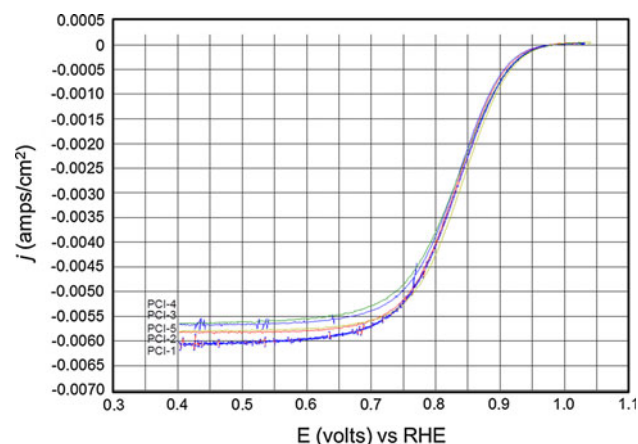Study by Gasteiger et al. is listed in Table 4 for comparison [13]:

Fig. 9 Potentiodynamic (5 mV s^{-1}) oxygen reduction current densities on a RSDT manufactured RDE spinning at 1600 rpm in an O$_2$ saturated 0.1 M HClO$_4$ electrolyte at 30 °C
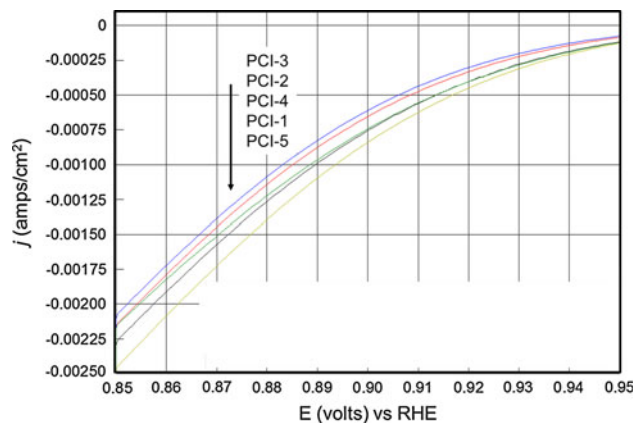
Fig. 10 Expanded view of potentiodynamic (5 mV s^{-1}) oxygen reduction current densities on a RSDT manufactured RDE spinning at 1600 rpm in an O$_2$ saturated 0.1 M HClO$_4$ electrolyte at 30 °C
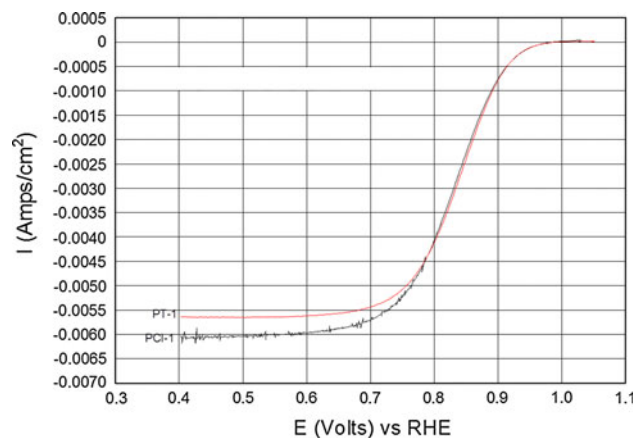
Fig. 11 Expanded view of potentiodynamic (5 mV s^{-1}) oxygen reduction current densities for a RSDT platinum only, RSDT composite, and TKK RDE spinning at 1600 rpm in an O$_2$ saturated 0.1 M HClO$_4$ electrolyte at 30 °C

It should be noted that the ORR conditions measured in the Gasteiger work were done at 60 °C versus 30 °C in this work. However, the diffusion limited current densities are predicted to remain nearly constant in this temperature range [14]. The data in Table 2 indicates that the RSDT electrodes show ECA's above those for the ink-prepared electrodes. Additionally, the mass activity for the PT-1 sample, 201 A/mg$_{Pt}$, is essentially equivalent to those for the ink samples whereas the specific activity, 220 µA/cm$^2_{Pt}$ is higher than all but the 20% Pt/Vu (ETEK) sample. The RSDT composite sample PCI-1 shows an ECA above all of the ink-prepared samples except for the 27% Pt/Ketjen but suffers a ~25% reduction in both mass and specific activity. The loading on the RSDT samples is about a half to a third of the loading on the ink-prepared samples so a better comparison would be a study with equivalent loadings.

Table 4 A comparison of electrochemical data for ink-prepared electrodes as reported by Gasteiger et al. [13] to electrodes synthesized in this work

	L_{Pt} $\mu g_{Pt}/cm^2$	ECA m^2_{Pt}/g_{Pt}	i_s @ 0.9 V mA/cm^2_{Pt}	i_m @ 0.9 V A/mg_{Pt}
ink prepared				
40% Pt/Vu (ETEK)	13.7	31	190	190
20% Pt/Vu (ETEK)	14.3	65	230	230
45.9% Pt/HSC-E (TKK)	12.7	78	190	190
27% Pt/Ketjen	16.1	120	150	200
RSDT				
PT-1	4.9	92	220	201
PCI-1	6.1	120	152	143

Conclusion

The RSDT technique is a viable method of dry depositing in one-step a low platinum loading or carbon supported platinum electrode that exhibits activity towards the oxygen reduction reaction without any post processing. The technique decouples the platinum, carbon and ionomer components which are constrained in ink-based processing methods. The best performing sample as determined by ECA and mass activity was with platinum deposited as a high surface area thin film without any carbon support or ionomer. The mass activity was 201 A/mg_{Pt} and the specific activity was 220 $\mu A/cm^2_{Pt}$. Platinum, without binder, forms a very thin layer porous layer on the electrode that is just as electrochemically accessible as the dispersed platinum as indicated by the ECA of 92 m^2/g. For the composite samples, the best performing sample had a lower ionomer to carbon ratio of ~ 0.5 compared to the other electrodes that had ratios of ~ 0.8. The mass activity of this composite was 143 A/mg_{Pt} and the specific activity was 152 $\mu A/cm^2_{Pt}$.

References

1. Choi ID, Lee H, Shim Y, Lee D (2010) Langmuir 26(13):11212
2. Ernst FO, Buchel R, Strobel R, Pratsinis S (2008) Chem Mater 20(6):2117
3. Strobel R, Pratsinis S (2007) J Mater Chem 17(45):4743
4. Mädler L, Roessler A, Pratsinis S, Sahm T, Gurlo A, Barsan N, Weimar U (2006) Sens Actuators B Chem 114(1):283
5. Maric R, Schalchi B, Mitlin D, Roller J, Neagu R (2010) Meet Abstr Electrochem Soc 1001(9):599
6. Roller J, Neagu R, Xie Z, Maric R (2010) Meet Abstr Electrochem Soc 1001(9):580
7. Xie Z, Haldane M, Roller J, Neagu R, Maric R, Navessin T, Holdcroft S (2010) Meet Abstr Electrochem Soc 1001(9):616
8. Roller J, Neagu R, Maric R, Xie Z (2009) Meet Abstr Electrochem Soc 902(10):1152
9. Maric R, Roller J, Neagu R, Fatih K, Tuck A (2008) ECS Trans 12(1):59
10. Roller J (2009) Low platinum electrodes for proton exchange fuel cells manufactured by reactive spray deposition technology. Dissertation, University of British Columbia
11. Maric R, Roller J, Neagu R (2011) J Therm Spray Technol 20(4):696
12. Paulus U, Schmidt T, Gasteiger H, Behm R (2001) J Electroanal Chem 495(2):134
13. Schmidt T, Gasteiger H, Stab G, Urban P, Kolb D, Behm R (1998) J Electrochem Soc 145(7):2354
14. Garsany Y, Baturina O, Swider-Lyons K, Kocha S (2010) Anal Chem 82(15):6321
15. Starz K, Auer E, Lehmann T, Zuber R (1999) J Power Sources 84(2):167
16. Eikerling M, Malek K, Wang Q (2008) In: Zhang J (ed) PEM fuel cell electrocatalysts and catalyst layers: fundamentals and applications, 1st edn. Springer, London, p 381